JOURNAL OF AIRCRAFT
Vol. 40, No. 4, July–August 2003

# Wing Optimization Using Design of Experiment, Response Surface, and Data Fusion Methods

A. J. Keane*
*University of Southampton, Highfield, Southampton, England SO17 1BJ, United Kingdom*

**An empirical drag prediction model plus design of experiment, response surface, and data-fusion methods are brought together with computational fluid dynamics (CFD) to provide a wing optimization system. This system allows high-quality designs to be found using a full three-dimensional CFD code without the expense of direct searches. The metamodels built are shown to be more accurate than the initial empirical model or than simple response surfaces based on the CFD data alone. Data fusion is achieved by building a response surface kriging of the differences between the two drag prediction tools, which are working at varying levels of fidelity. The kriging is then used with the empirical tool to predict the drags coming from the CFD code. This process is much quicker to use than direct searches of the CFD.**

## Introduction

THE Southampton multilevel wing design environment[1] is used to study the merits of data fusion when applied to three-dimensional computational fluid dynamics (CFD) solvers over a transonic wing system. The aim is to build a multifidelity response surface model (RSM) using both empirical and CFD data to model variations in drag at fixed lift as gross changes are made to the overall wing parameters. Currently, such changes are usually assessed using empirical concept design tools that make no attempt to solve the flow conditions over the wings being studied. Although these concept tools can be extremely accurately calibrated to deal with familiar geometries, they experience difficulties whenever extreme or even moderately novel configurations are considered. They are, however, very easy to use and are capable of giving rapid estimates of likely drag levels.[2]

It would, of course, be useful if full three-dimensional CFD solvers could be used in lieu of the empirical codes contained in normal concept tools: Currently this is not standard practice because of two major difficulties. First, empirical concept tools do not require complete geometric details of the wing being studied because they typically work with gross wing parameters such as aspect ratio, span, mean camber, etc., whereas CFD solvers of course require a complete surface and mesh description. Such descriptions can be quite time consuming to develop to sufficient levels of realism to be of use in practical applications. Second, even Euler-based CFD codes typically have quite lengthy run times when considering three-dimensional geometries. The Southampton multilevel wing design environment addresses the first of these concerns: It allows designers to generate complete geometric descriptions of transonic wings, together with suitable CFD meshes from the limited set of gross wing parameters usually available to concept designers. This process mimics the process of wing design usually undertaken by specialist aerodynamics divisions and makes use of orthogonal airfoil section data to build a suitable cambered, twisted, tapered wing that meets the user's requirements.[3,4]

The system as originally described, however, did not offer much to mitigate problems of run time. All that was proposed in the original system was that designers should start work with the concept tools usually available and then switch to the full CFD solver whenever sufficient progress had been made. The ability to make this switch without supplying extra geometric data was its main advance. Therefore, for example, when carrying out an optimization study, initial searches would be made using the empirical concept tool, and these designs could then be seamlessly passed to the Euler solver for further, less wide-ranging, and necessarily shorter searches. Although this approach was a step forward, it is not of great benefit during design synthesis because most of the design tradeoffs considered are still made with the empirical code. Rather, it is most useful to check rapidly that the empirical methods of the original concept tool are still valid at any more radical design points of interest.

The work reported here attempts to overcome this limitation by fusing together data coming from empirical and CFD-based drag routines using design of experiment (DOE) techniques[5,6] and kriging[7] to build RSMs.[8] Variants on these methods have been used in aerospace design for some time. However, thus far they have mostly been used to accelerate direct optimization approaches using expensive codes.[9] It is only relatively recently that it has been proposed that they might be helpful in multilevel analysis (sometimes termed multifidelity or zoom analysis).[10–14] The main aim in multilevel analysis is to use the DOE and kriging to produce an RSM that models corrections to the low-cost, empirical analysis so that the correction model, together with the drag model of the original concept tool, may be used in lieu of the full CFD code. This provides results that are both well calibrated and capable of being used outside of the scope of the original concept tool in a seamless fashion. The basic approach for this kind of multifidelity modeling is described in more detail elsewhere[15]; here the aim is to demonstrate its application to a modern wing design problem using the latest approximation techniques and to illustrate its potential benefits and shortcomings in this relatively realistic setting. See the original reference 15 for a more complete description of the approach using low-order polynomials.

The techniques described here have recently been incorporated within the OPTIONS design exploration system, and the results presented have been produced using that system to drive the Southampton wing design environment (Keane, A. J., "The OPTIONS Design Exploration System User Guide and Reference Manual," http://www.soton.ac.uk/~ajk/options.ps [cited May 2001]).

## Example and Some Basic Searches

Before a discussion of multilevel approaches is commenced, it is useful to illustrate briefly the use of the wing design environment for direct searches, using either the empirical or CFD solvers. Here the response being studied is the drag of a transonic civil transport wing. A simple test problem has been constructed with the aim of

Received 16 May 2002; revision received 22 October 2002; accepted for publication 23 October 2002. 

*Professor, Computational Engineering, and Director, BAE Systems/Rolls–Royce University Technology Partnership for Design Search and Optimisation, School of Engineering Sciences.

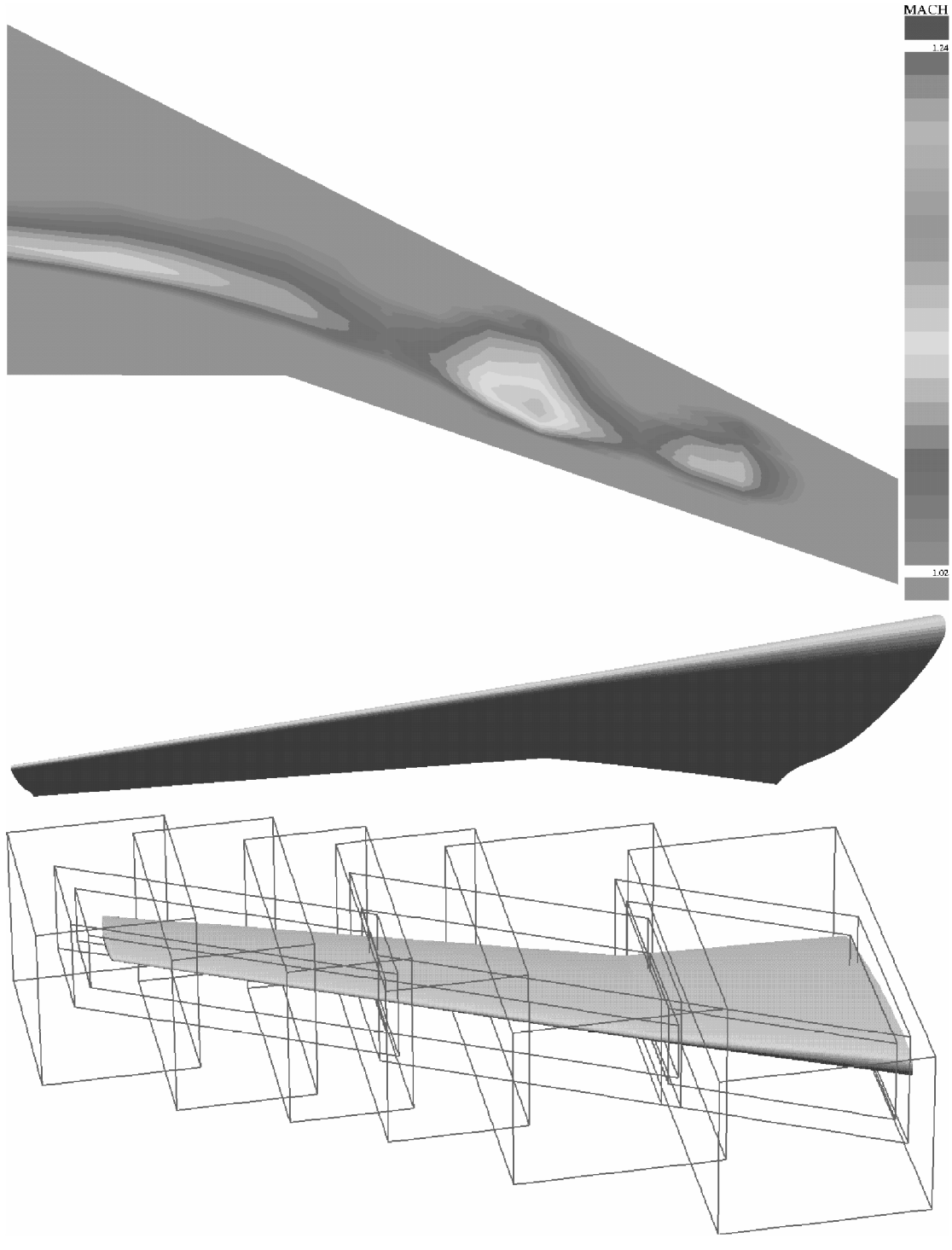


**Fig. 1 Initial wing geometry and overall CFD meshing (plan view shows upper surface supersonic Mach contours).**

optimizing the wing for operation at Mach 0.785 and a Reynolds number of $7.3 \times 10^6$. The objective is minimization of wing $D/q$ as calculated by the CFD solver with target lift, wing weight, volume, pitch-up margin, and root triangle layout chosen to be representative of a 220-seat wide-body airliner. Limits are placed on the design variables that are typical of work in this area. (Although they still admit designs that would be considered radical in practice, it is not common to use sweep angles as high as 45 deg in a civil aircraft, for example.)

The drag is computed either using the Tadpole concept design tool developed by the former Airbus division of BAE Systems[2] or by using the commercial MGAERO CFD code, which is a viscous coupled Euler solver.[16] In the latter case, a series of drag recovery routines are incorporated to assess the various drag components in a fashion compatible with the Tadpole concept tool. The input geometries to the CFD solver are created using a set of orthogonal functions derived from NACA transonic foils.[3,4] Typically the Tadpole analysis takes a few seconds, whereas the Euler analysis may require up to 2 h on a 1-GHz Pentium III processor. Typical results from these two systems are detailed in Table 1, and Fig. 1 shows the equivalent geometry. Notice that in this case the wing is defined by 11 parameters and also that constraints are placed on the wing volume, undercarriage bay length, pitch-up margin, and weight. At all times, the angle of attack is set to generate the required lift, and the wing weight changes in a realistic fashion allowing for necessary structural modifications as its dimensions alter. Here, the two

**Table 1 Initial design parameters, constraint values, and objective function values**

| Lower limit | Value | Upper limit | Quantity |
|---|---|---|---|
| 100 | 168 | 250 | Wing area, $m^2$ |
| 6 | 9.07 | 12 | Aspect ratio |
| 0.2 | 0.313 | 0.45 | Kink position |
| 25 | 27.1 | 45 | Sweep angle, deg |
| 0.4 | 0.598 | 0.7 | Inboard taper ratio |
| 0.2 | 0.506 | 0.6 | Outboard taper ratio |
| 0.1 | 0.150 | 0.18 | Root $t/c$ |
| 0.06 | 0.122 | 0.14 | Kink $t/c$ |
| 0.06 | 0.122 | 0.14 | Tip $t/c$ |
| 4.0 | 4.5 | 5.0 | Tip washout, deg |
| 0.65 | 0.75 | 0.84 | Kink washout fraction |
| | 127,984 | 135,000 | Wing weight, N |
| 40.0 | 41.73 | | Wing volume, $m^3$ |
| | 4.179 | 5.4 | Pitch-up margin |
| 2.5 | 2.693 | | Undercarriage bay length, m |
| | 3.145 | | Tadpole $D/q$, $m^2$ |
| | 2.922 | | MGAERO $D/q$, $m^2$ |

methods yield drag estimates that differ by some 8% despite the careful validation of the Tadpole code and considerable effort in attempting to get the drag recovery from the Euler code to work in a directly compatible fashion.[17–19] This is partially due to the public domain wing airfoil sections used to generate the CFD geometry, which differ from the commercial sections for which Tadpole is calibrated.

After this simplified design problem is set up, it may then be very rapidly optimized if the empirical code is used to estimate the drag. Here a 25-generation genetic algorithm (GA) search with a population size of 200 members has been used[20] followed by a gradient descent search to fine tune the final optimum.[21,22] Note that GAs are not deterministic in nature and rely on the random number sequences being used. When such stochastic search engines are tested or developed, it is, therefore, normal practice to average results over a number of statistically independent trials: When they are used in design, this is a luxury that rarely can be afforded. Here each GA search is carried out for just one set of random numbers. Therefore, some caution must be exercised when considering the results, particularly those that depend on single, relatively short GA searches. The results are more certain where several such searches are combined in producing designs (such as when using the multiple updates that will be described later) or when rather longer GA searches with larger populations can be afforded (as here for the Tadpole search).

The GA used is fairly conventional except that it incorporates a version of MacQueen's adaptive KMean algorithm (see Ref. 23), a clustering algorithm that has been applied with some success to multipeak problems.[24] It works with 12-bit binary encoding, an elitist survival strategy that ensures that the best of each generation always enters the next generation, five major control parameters, a one-pass external constraint penalty function, and optional niche forming.

The main control parameters used in this GA are $P$ [best], the proportion of the population that survives to the next generation (default 0.8); $P$ [cross], the proportion of the surviving population that is allowed to breed (default 0.8); $P$ [invert], the proportion of the surviving population that have their genetic material reordered (default 0.5); $P$ [mutation], the proportion of the new generation's genetic material that is randomly changed (default 0.005); and a proportionality flag that selects whether the new generation is biased in favor of the most successful members of the previous generation or alternatively if all $P$ [best] survivors are propagated equally. (Default is to bias in favor of successful members.)

The version of the adaptive KMean algorithm used is controlled by $D_{\min}$, the minimum nondimensional Euclidean distance between cluster centers, with clusters closer than this being collapsed (default 0.1); $D_{\max}$, the maximum nondimensional Euclidean radius of a cluster, beyond which clusters subdivide (default 0.2); $N_{\text{clust}}$, the initial number of clusters into which a generation is divided (default 25); $N_{\text{breed}}$, the minimum number of members in a cluster before exclusive inbreeding within the cluster takes place (default 5); and $\alpha$, the penalizing index for cluster members that determines how severely members sharing an overcrowded niche will suffer, with small numbers giving less penalty, that is, the objective functions of members of a cluster of $m$ solutions are scaled by $m^{\min(\alpha,1)}[1 - (E/D_{\max})^{\alpha}] + (E/D_{\max})^{\alpha}$, where $E$ is the Euclidean distance of the member from its cluster center, which is always less than $D_{\max}$. Moreover, when $E = D_{\max}$ or $\alpha = 0$, no penalty is applied (default $\alpha = 0.5$).

Like all evolutionary methods, the GA is rather slow and inaccurate for problems with few variables but comes into its own as the number of variables grows. It is also not suitable for problems without bounds on all of the variables. Currently, GAs seem to the best of the commonly used stochastic methods. Because of these limitations, where possible the GA is followed up by a traditional downhill search, normally the well-known simplex method,[21] but if this stalls, which it sometimes does, by Rosenbrock's rotating coordinate search.[22]

Application of this hybrid GA/downhill optimization strategy to the Tadpole code drives the wing volume constraint down to its limit and also increases the sweep angle considerably, although the total wing area is little changed (Table 2). This reduces the drag by over 9% (as predicted by Tadpole). Such a search process represents the current everyday activity of a concept design team. After this study is carried out, the Southampton system then allows the drag to be checked by invoking the CFD solver. This result is also recorded in Table 2, and it is seen that again the predictions still differ, now by 12%. The CFD-predicted drag has, however, been decreased by nearly 13%.

Given the difference in drag between the two predictions, it is interesting to check whether a direct search applied to the CFD code would have produced a similar design geometry. Table 3 gives the results of such a study, although now the GA optimization has been reduced to 15 generations and a population size of only 100, and the final hill-climbing search has been omitted, all to save time. Even so, this search represents some 150 days of computing effort; here carried out on a cluster of personal computers running in parallel over two weeks. (The Tadpole search took 10 minutes.) The extreme cost of such searches makes them infeasible for everyday use, but they do provide benchmarks against which to compare other results. Notice that in this case the drag is reduced by some 14% (as predicted by the Euler CFD code) and that the two codes still do not agree on the resulting drag, now differing by 19%. When Tables 2 and 3 are compared, it is apparent that the two methods converge to somewhat different optima for this design study. The Tadpole-predicted drag in Table 3 is nearly 5% higher than that in Table 2, whereas the CFD-predicted drag is slightly more than 1% lower. Moreover, the CFD-based wing has a significantly larger area.

**Table 2 Final design parameters, constraint values, and objective function values for the best design produced by the direct Tadpole search**

| Lower limit | Value | Upper limit | Quantity |
|---|---|---|---|
| 100 | 168.5 | 250 | Wing area, $m^2$ |
| 6 | 9.32 | 12 | Aspect ratio |
| 0.2 | 0.244 | 0.45 | Kink position |
| 25 | 31.8 | 45 | Sweep angle, deg |
| 0.4 | 0.516 | 0.7 | Inboard taper ratio |
| 0.2 | 0.227 | 0.6 | Outboard taper ratio |
| 0.1 | 0.104 | 0.18 | Root $t/c$ |
| 0.06 | 0.115 | 0.14 | Kink $t/c$ |
| 0.06 | 0.063 | 0.14 | Tip $t/c$ |
| 4.0 | 4.7 | 5.0 | Tip washout, deg |
| 0.65 | 0.68 | 0.84 | Kink washout fraction |
| | 133,895 | 135,000 | Wing weight, N |
| 40.0 | 40.0 | | Wing volume, $m^3$ |
| | 5.04 | 5.4 | Pitch-up margin |
| 2.5 | 3.51 | | Undercarriage bay length, m |
| | 2.853 | | Tadpole $D/q$, $m^2$ |
| | 2.555 | | MGAERO $D/q$, $m^2$ |

**Table 3 Final design parameters, constraint values, and objective function values for the best design produced by the direct MGAERO search**

| Lower limit | Value | Upper limit | Quantity |
|---|---|---|---|
| 100 | 177.5 | 250 | Wing area, $m^2$ |
| 6 | 9.30 | 12 | Aspect ratio |
| 0.2 | 0.406 | 0.45 | Kink position |
| 25 | 25.2 | 45 | Sweep angle, deg |
| 0.4 | 0.683 | 0.7 | Inboard taper ratio |
| 0.2 | 0.259 | 0.6 | Outboard taper ratio |
| 0.1 | 0.143 | 0.18 | Root $t/c$ |
| 0.06 | 0.096 | 0.14 | Kink $t/c$ |
| 0.06 | 0.069 | 0.14 | Tip $t/c$ |
| 4.0 | 4.5 | 5.0 | Tip washout, deg |
| 0.65 | 0.67 | 0.84 | Kink washout fraction |
| | 130,166 | 135,000 | Wing weight, N |
| 40.0 | 41.6 | | Wing volume, $m^3$ |
| | 3.67 | 5.4 | Pitch-up margin |
| 2.5 | 2.56 | | Undercarriage bay length, m |
| | 2.998 | | Tadpole $D/q$, $m^2$ |
| | 2.524 | | MGAERO $D/q$, $m^2$ |

These results demonstrate the power of the Southampton wing design system to explore interesting geometries. It is, however, noticeable that the difference in drag estimation between the two approaches has risen significantly after the searches and that they converge toward different geometries. Presumably the differences in drag in Table 3 arise because the empirical code is then working rather far away from the calibrated zones for which it has been extensively tested.

## RSM

The searches reported in the preceding section simply involved applying optimization methods directly to the analysis codes, in this case using a GA for wide-ranging searches and then downhill methods for local improvement, if they can be afforded. (Recall that downhill methods cannot normally make great use of parallel computing environments.) Even with parallel computing, searches on the full Euler code are still very expensive to carry out. Consequently, many workers in this field advocate the use of RSMs where surrogate metamodels are produced by curve-fitting techniques to samples of the expensive data.[7,8]

The basic RSM process involves selecting a limited number of points at which the expensive code will be run, normally using formal DOE methods.[5,6] Then, when these designs have been analyzed, usually in parallel, a response surface (curve fit) is constructed through or near the data. Design optimization is then carried out on this surface to locate new and interesting combinations of the design variables, which may then, in turn, be fed back into the full code. These data can then be used to update the model and the whole process repeated until the user either runs out of effort, some form of convergence is achieved, or sufficiently improved designs are reached. This process is shown in Fig. 2.

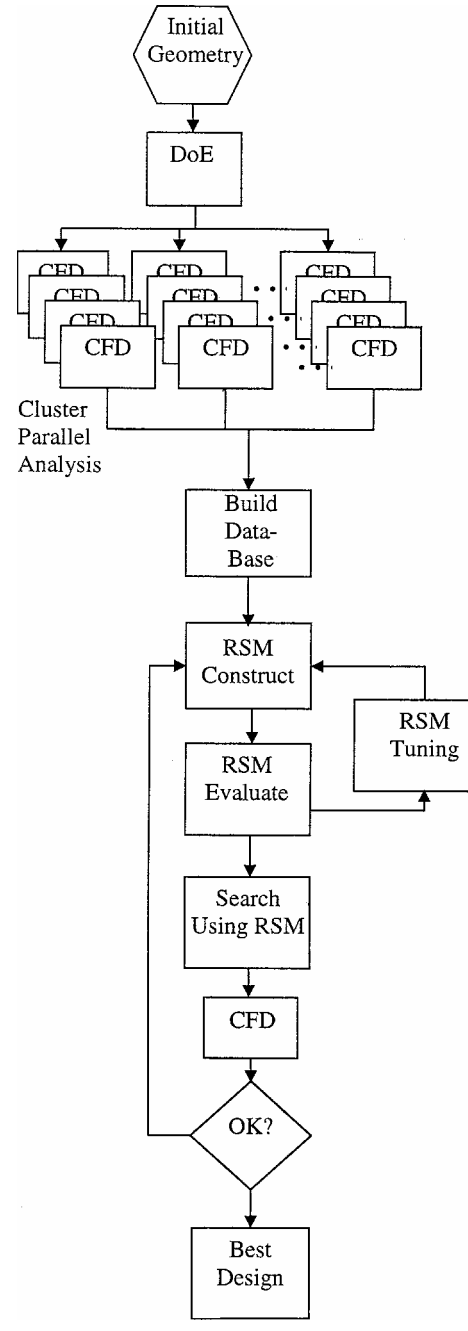


**Fig. 2 RSM-based optimization strategy.**

## DOE Methods and Kriging

It is no surprise that there are a number of variations and refinements that may be applied to the basic RSM approach. The literature offers many possible alternatives. Here, by way of example, an LP$\tau$ DOE sequence[25] is used to generate the initial set of points and a kriging model applied to build the RSM.[7]

Most DOE methods seek to sample efficiently the entire design space by building an array of possible designs with relatively even but not constant spacing between the points. Notice that this is in contrast to a pure random spacing, which would result in some groups of points occurring in clumps, whereas there were other regions with relatively sparse data. This might be desirable if there were no correlation between the responses at points, however close they were to each other, that is, the process resembled white noise, but this is highly unlikely in engineering design problems. A particular advantage of the LP$\tau$ approach is that not only does it give good coverage for engineering purposes, but that it also allows additional points to be added to a design without the need to reposition existing points. This can be useful if the designer is unsure how many points will be needed before commencing work. Then, if the initial build of the RSM is found to be inadequate, a new set of points can be inserted without invalidating the statistical character of the experiment. (Similarly, if for some reason the original experiment cannot be completed, the sequence available at any intermediate stage will still have useful coverage.)

After an array of data points is built up from which a surface can be constructed, the user's next major decision is whether or not to regress (as opposed to interpolate) the data. Regression of course allows for noise in the data (which may occur due to convergence errors in CFD, for example) but also allows the response surface to model rapidly changing data without excessive curvature. Consider trying to fit a polynomial to a function like a square wave. It is well known that such curve fits typically have difficulty modeling the steps in the function without overshoot if they are forced to

interpolate the data points. In such circumstances, a degree of regression may give a more useful model, particularly when optimization searches are then applied to the problem because functions using regression usually have fewer basins of attraction and are, thus, easier to search.

The most obvious forms of regression are those using least-squares (often quadratic) polynomials. These are commonly used in the statistics community, and much of the RSM literature is based on them. They are not good, however, at modeling complex surfaces that have many local basins and bulges in them. Here a kriging approach is used instead[7] because this allows the user to control the amount of regression as well as providing a theoretically sound basis for judging the degree of curvature needed to model adequately the user's data. Additionally, kriging provides measures of probable errors in the model being built that can be used when assessing where to place any further design points. It also allows for the relative importance of variables to be judged.

In kriging, the inputs $\boldsymbol{x}$ are assumed to be related to the outputs (responses) $y$ by an expensive function $f_e(\boldsymbol{x})$. Here this function is the MGAERO Euler CFD code drag prediction. The response of the code is then evaluated for combinations of inputs generated by the DOE and used to construct an approximation,

$$y = f_e(\boldsymbol{x}) \tag{1}$$

The response at any $\boldsymbol{x}$ is then approximated by

$$y = \mu + \varepsilon(\boldsymbol{x}) \tag{2}$$

where $\mu$ is the mean of the input responses and $\varepsilon(\boldsymbol{x})$ is a Gaussian random function with zero mean and variance $\sigma^2$. In kriging, $\varepsilon$ is taken to depend on the distance between corresponding points. The distance measure used here is

$$d\left(\boldsymbol{x}^{(i)}, \boldsymbol{x}^{(j)}\right) = \sum_{h=1}^{k} \theta_h \left(x_h^{(i)} - x_h^{(j)}\right)^{p_h} \tag{3}$$

where $\theta_h$ and $p_h$ are hyperparameters tuned to the data in hand. The correlation between points $\boldsymbol{x}^{(i)}$ and $\boldsymbol{x}^{(j)}$ is given by

$$\boldsymbol{R}\left(\boldsymbol{x}^{(i)}, \boldsymbol{x}^{(j)}\right) = \exp\left[-d\left(\boldsymbol{x}^{(i)}, \boldsymbol{x}^{(j)}\right)\right] + \Lambda\delta_{ij} \tag{4}$$

where $\Lambda$ is a regularization constant that governs the degree of regression in the model and $\delta_{ij}$ is the Dirac delta function. (When set to zero, the kriging strictly interpolates the data supplied.) When the response at a new point $\boldsymbol{x}$ is required, a vector of correlations between the point and those used in the DOE is formed, $\boldsymbol{r}(\boldsymbol{x}) = \boldsymbol{R}(\boldsymbol{x}, \boldsymbol{x}^{(i)})$. The prediction is then given by

$$y(\boldsymbol{x}) = \mu + \boldsymbol{r}^T\boldsymbol{R}^{-1}(\boldsymbol{y} - \mathbf{1}\mu) \tag{5}$$

where the mean $\mu$ is found from

$$\mu = \mathbf{1}^T\boldsymbol{R}^{-1}\boldsymbol{y}/\mathbf{1}^T\boldsymbol{R}^{-1}\mathbf{1} \tag{6}$$

The hyperparameters $\theta_h$ and $p_h$ and regularization constant $\Lambda$ are all obtained by maximizing the likelihood, defined as

$$\frac{1}{(2\pi)^{N/2}(\sigma^2)^{N/2}|\boldsymbol{R}|^{\frac{1}{2}}} \exp\left[\frac{-(\boldsymbol{y} - \mathbf{1}\mu)^T\boldsymbol{R}^{-1}(\boldsymbol{y} - \mathbf{1}\mu)}{2\sigma^2}\right] \tag{7}$$

where the variance $\sigma^2$ is given by

$$\sigma^2 = (\boldsymbol{y} - \mathbf{1}\mu)^T\boldsymbol{R}^{-1}(\boldsymbol{y} - \mathbf{1}\mu)/N \tag{8}$$

$N$ is the number of points used in the DOE. The mean-squared error of the prediction is

$$s^2(\boldsymbol{x}) = \sigma^2\left[1 + \boldsymbol{r}^T\boldsymbol{R}^{-1}\boldsymbol{r} + \frac{(1 - \mathbf{1}^T\boldsymbol{R}^{-1}\boldsymbol{r})^2}{\mathbf{1}^T\boldsymbol{R}^{-1}\mathbf{1}}\right] \tag{9}$$

which gives a measure of the accuracy of the kriging at $\boldsymbol{x}$. One of the attractions of kriging is that the $\theta$ hyperparameters produced may be used to screen the variables in the data for relative importance if the input variables are normalized to a unit range before the kriging is tuned. Once tuned, the hyperparameters simply rank the significance of the variables they represent.

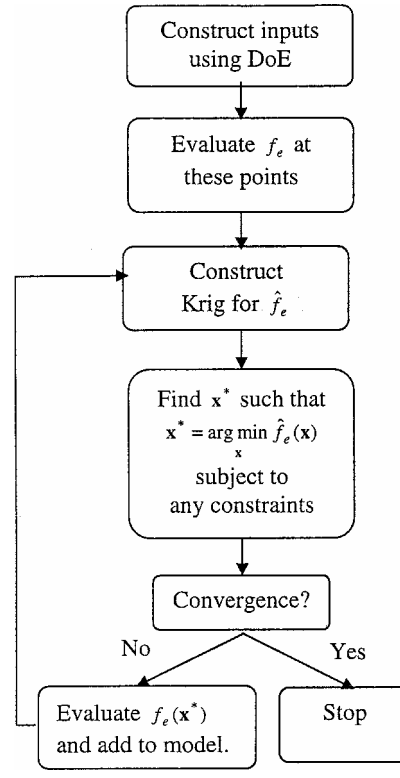


**Fig. 3 Kriging procedure for function $f_e$.**

This basic approach can be used to model any response quantity, including constraints. Here, because the constraints may be rapidly computed, there is no need to apply the RSM process to them at all. (In the studies reported, empirical structural and weight models are used for the calculations underlying the constraints.) Thus, a kriging is built just for the predicted drag. The general strategy is shown in Fig. 3.

However, kriging is not a panacea for all evils. It is commonly found that it is difficult to set up such models for more than 10–20 variables and also that the approach is numerically expensive if there are more than a few hundred data points because the setup (hyperparameter tuning) process requires the repetitive lower–upper (LU) decomposition of the correlation matrix $\boldsymbol{R}$, which has the same dimensions as the number of points used. Moreover, the number of such LU steps is strongly dependent on the number of variables, and the likelihood is commonly highly multimodal. The author has found that it is difficult to deal with kriging involving more than 15 variables and 500 data points.

## Application of DOE and Kriging

To demonstrate basic RSM production, 250 points of an LP$\tau$ array have been applied to the example problem of Table 1, which has 11 variables, using the inexpensive Tadpole code and a kriging built using a GA and a gradient descent two-stage search of the concentrated likelihood function to tune the hyperparameters. (See Table 4 and note that $\log_{10}(\theta)$ hyperparameter values less than $-2$ indicate variables with relatively little impact on the kriging. Here, the dominant variables are, therefore, wing area, aspect ratio, sweep angle, and inboard taper ratio.) To demonstrate the accuracy of this model, 390 further random design points were also computed with Tadpole, and then the results at these further points were predicted using kriging. Figure 4 shows the correlation plot for this test data, and it may be seen that, although some differences occur, the overall correlation coefficient is 0.991. This relatively good predictive capability is also indicated by a standardized cross-validated (SCV)

**Table 4 Kriging hyperparameters for Tadpole model with 11 variables produced from 250 LP$\tau$ data points[a]**

| $\text{Log}_{10}(\theta)$ | $p_h$ | Quantity |
|---|---|---|
| _0.593 | 1.573 | Wing area |
| _1.428 | 1.826 | Aspect ratio |
| _2.294 | 1.778 | Kink position |
| _0.910 | 1.443 | Sweep angle |
| _1.574 | 1.569 | Inboard taper ratio |
| _2.006 | 1.596 | Outboard taper ratio |
| _2.177 | 1.824 | Root $t/c$ |
| _2.320 | 2.000 | Kink $t/c$ |
| _2.472 | 1.352 | Tip $t/c$ |
| _8.615 | 1.886 | Tip washout |
| _2.761 | 1.468 | Kink washout fraction |

[a]Regularization constant = $10^{-18}$.

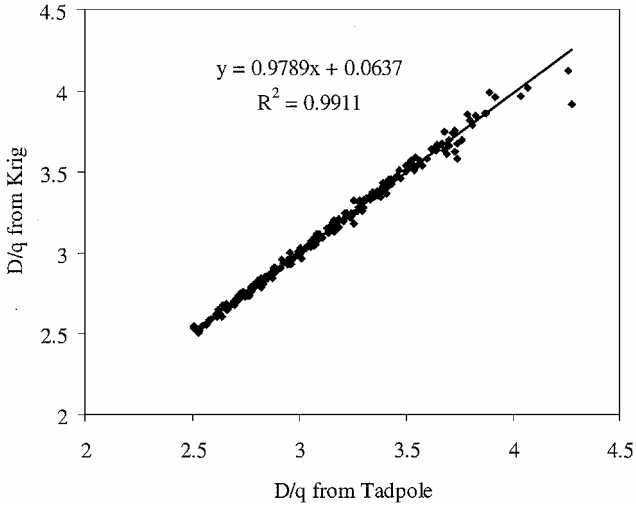


**Fig. 4 Correlation between 390 random Tadpole *D/q* calculations and those predicted by the Kriging trained on a separate set of 250 LP$\tau$ calculations.**

residual test on the original data, where the mean SCV residual turns out to be 0.541 with just two of the 390 residuals being greater than 3. (Values of less than 1 represent a good model, whereas those over 3 indicate poor correlations, that is, outliers.) Moreover, negligible regularization (regression) is needed to model the data.

These results show that it is possible to build kriging successfully with this many dimensions using 250 data points. This is hardly necessary for Tadpole given its run time, however, which is barely more than that for using the kriging itself. Moreover, tuning the hyperparameters for this model takes much longer than the generation of the original Tadpole data. The real use of the approach arises when attempting to model expensive data coming from the CFD code itself. This process is not so successful because the CFD data are intrinsically much less smooth and contain significant noise. Table 5 and Fig. 5 show an equivalent set of results for a kriging built on CFD data, which yields a correlation coefficient of only 0.4903. It is clear from Fig. 5 that there is much more scatter in these results, fortunately, mostly for the higher drag data. With this model, the mean SCV is 0.929, and now 10 residuals are greater than 3, again indicating that these data are harder to model with many more outliers. Significant regularization is also required. Note further that the relative significances of the variables have changed between Tables 4 and 5. In Table 5, the sweep angle is seen to be much less important than in Table 4, whereas two of the thickness to chord ratios and the kink washout fraction are more important. In Tables 4 and 5, the wing area, aspect ratio, and inboard taper ratio remain significant.

Of course, the real test for the kriging of the MGAERO data is whether or not they can be successfully used to optimize the wing design as predicted by the CFD code. Thus, next a two-stage GA and gradient descent search has been carried out on the kriging RSM and the resulting design evaluated with the CFD code (and Tadpole for

**Table 5 Kriging hyperparameters for MGAERO model with 11 variables produced from 250 LP$\tau$ data-points[a]**

| $\text{Log}_{10}(\theta)$ | $p_h$ | Quantity |
|---|---|---|
| _0.866 | 1.718 | Wing area |
| _1.698 | 1.983 | Aspect ratio |
| _8.228 | 1.513 | Kink position |
| _2.108 | 1.001 | Sweep angle |
| _0.282 | 1.004 | Inboard taper ratio |
| _3.782 | 2.000 | Outboard taper ratio |
| _1.848 | 2.000 | Root $t/c$ |
| _0.967 | 1.830 | Kink $t/c$ |
| _2.854 | 1.012 | Tip $t/c$ |
| _3.293 | 1.749 | Tip washout |
| _1.668 | 2.000 | Kink washout fraction |

[a]Regularization constant = $1.22 \times 10^{-2}$.

**Table 6 Design parameters, constraint values, and objective function values for the best design produced by the search on the initial MGAERO kriging**

| Lower limit | Value | Upper limit | Quantity |
|---|---|---|---|
| 100 | 169.7 | 250 | Wing area, $m^2$ |
| 6 | 8.135 | 12 | Aspect ratio |
| 0.2 | 0.411 | 0.45 | Kink position |
| 25 | 30.74 | 45 | Sweep angle, deg |
| 0.4 | 0.471 | 0.7 | Inboard taper ratio |
| 0.2 | 0.309 | 0.6 | Outboard taper ratio |
| 0.1 | 0.117 | 0.18 | Root $t/c$ |
| 0.06 | 0.0732 | 0.14 | Kink $t/c$ |
| 0.06 | 0.103 | 0.14 | Tip $t/c$ |
| 4.0 | 4.005 | 5.0 | Tip washout, deg |
| 0.65 | 0.849 | 0.84 | Kink washout fraction |
| | 134,920 | 135,000 | Wing weight, N |
| 40.0 | 40.0 | | Wing volume, $m^3$ |
| | 4.14 | 5.4 | Pitch-up margin |
| 2.5 | 3.30 | | Undercarriage bay length, m |
| | 2.429 | | Kriging $D/q$, $m^2$ |
| | 3.046 | | Tadpole $D/q$, $m^2$ |
| | 2.777 | | MGAERO $D/q$, $m^2$ |

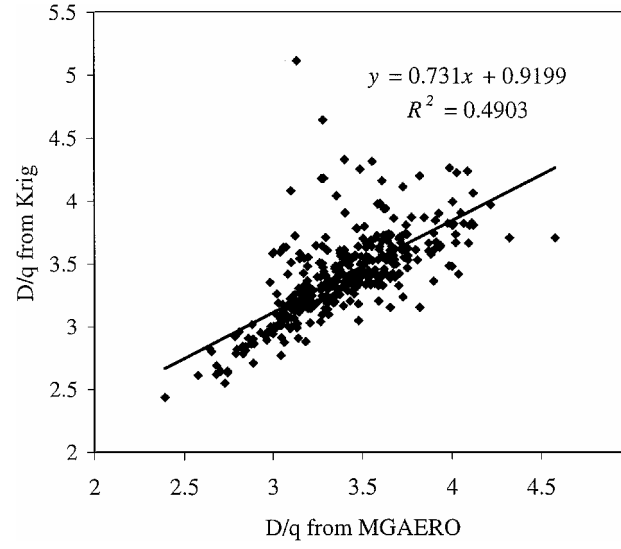


**Fig. 5 Correlation between 390 random MGAERO *D/q* calculations and those predicted by the Kriging trained on a separate set of 250 LP$\tau$ calculations.**

comparison) (Table 6). This design has significantly worse drag than either of those in Tables 2 or 3 using either Tadpole or MGAERO to predict the drag, despite the kriging predicting much lower drags for this design. Clearly kriging is not modeling the data well in this location. This is quite normal when dealing with problems in high dimensions because the initial DOE cannot be expected to give sufficient coverage in all possible areas of interest. This is why it is almost always necessary to update the data set used to build the

kriging by adding new points in areas where good designs are being predicted. (There are other schemes for positioning these added points such as the use of expected improvement criteria, but these are not discussed here; see Ref. 7 instead.)

Following the update strategy of Fig. 2, the design point of Table 6 is then added to the set used to produce the kriging, and the hyperparameters retuned before it is again used to try and find an improved design. This process can be repeated as many times as the designer wants or until some form of convergence is achieved. Here 10 such iterations are carried out to yield the result of Table 7. This final design, although better than the initial design, fails to give $D/q$ values as good as those achieved either by the direct search on the empirical Tadpole code, or on the Euler-based MGAERO CFD code. Its performance is 0.7% worse than the best design achieved by Tadpole optimization (and using Tadpole predictions for comparison) and 0.6% worse than that from the direct CFD optimization. This result indicates that, although the RSM approach commonly yields improved results, these may well not be as good as direct searches on the underlying codes. This can occur even when suitable steps are taken to update the surface as part of the process and represents a fundamental limitation of metamodeling. The approach is, however, much faster than the direct CFD search because it requires nearly six times fewer CFD evaluations.

Having shown what may be achieved with simple optimization and the direct response surface approach, attention is turned to fusion of the information coming from Tadpole and the MGAERO CFD runs. Here, this is termed multilevel analysis.

**Table 7 Final design parameters, constraint values, and objective function values for the best design produced by the search on the refined MGAERO kriging produced with 10 updates**

| Lower limit | Value | Upper limit | Quantity |
|---|---|---|---|
| 100 | 158.7 | 250 | Wing area, m$^2$ |
| 6 | 9.781 | 12 | Aspect ratio |
| 0.2 | 0.367 | 0.45 | Kink position |
| 25 | 30.18 | 45 | Sweep angle, deg |
| 0.4 | 0.467 | 0.7 | Inboard taper ratio |
| 0.2 | 0.300 | 0.6 | Outboard taper ratio |
| 0.1 | 0.133 | 0.18 | Root $t/c$ |
| 0.06 | 0.106 | 0.14 | Kink $t/c$ |
| 0.06 | 0.0627 | 0.14 | Tip $t/c$ |
| 4.0 | 4.838 | 5.0 | Tip washout, deg |
| 0.65 | 0.679 | 0.84 | Kink washout fraction |
| | 134,982 | 135,000 | Wing weight, N |
| 40.0 | 40.0 | | Wing volume, m$^3$ |
| | 4.99 | 5.4 | Pitch-up margin |
| 2.5 | 3.05 | | Undercarriage bay length, m |
| | 2.316 | | Kriging $D/q$, m$^2$ |
| | 2.879 | | Tadpole $D/q$, m$^2$ |
| | 2.543 | | MGAERO $D/q$, m$^2$ |

## Multilevel Analysis

With multilevel (multifidelity or zoom) analysis, it is assumed that the designer has at least two different ways of computing results of interest for the design under consideration. In Ref. 1, an optimization study was carried out using the Southampton multilevel wing design system by first applying a wide-ranging GA search to the empirical code and then using this to seed a much smaller search on the Euler code. The results of that study reduced the drag by some 17%, albeit for a slightly different example. (The weight and structural models used have since been refined for the work reported here, along with the constraints placed on them.) This improved on the use of a direct search applied to the CFD code alone by some 7%, because, despite the differences between the codes, sufficient improvement was achieved by the empirical method that the CFD-based search was able to capitalize on the better starting position. These results are reproduced in the columns of Table 8 for ease of reference. In both cases, the MGAERO searches were 1000-step GA optimizations (10 generations of 100 members).

Despite the improvement over a direct search, there remain two fundamental problems with this two-stage approach: 1) Unless the methods agree very well, there is a danger that the results coming from one may mislead the other. Such differences are apparent in all of the results in Tables 1–3 and 6–8. 2) The final direct search of the CFD code is still too computationally expensive for routine use. Clearly what would be preferable is a more sophisticated approach to integrating these sources of design information, that is, some kind of data fusion system.

This may be achieved if instead of using the RSM to model the expensive CFD code directly it is used to capture the differences between this and the cheaper empirical alternative. The RSM then serves as an online correction service to the empirical code so that, when designs are studied where it is less accurate, the corrections derived from full three-dimensional CFD are automatically included. To begin this process, data coming from the DOE run on MGAERO is taken, and an equivalent set of drag results is computed for each point, using Tadpole. The differences between the two are then used to form the kriging. Then, when searches are carried out and new predictions are needed, these are calculated by calling both Tadpole and the kriging and summing their contributions. Again the kriging is built using a GA and gradient descent two-stage search of the concentrated likelihood function to tune the hyperparameters. (See Table 9 and note that now the $\log_{10}(\theta)$ hyperparameters indicate the dominant differences in the effects of variables and that the sweep angle is the critical one here, that is, it is in the impact of sweep that the two codes differ most.)

**Table 8 Final design parameters, constraint values, and objective function values for the best designs produced by the two stage Tadpole/MGAERO and direct MGAERO searches[a]**

| Lower limit | Value (initial) | Value (two stage search) | Value (direct CFD search) | Upper limit | Quantity |
|---|---|---|---|---|---|
| 100 | 168 | 165.8 | 168 | 250 | Wing area, m$^2$ |
| 6 | 9.07 | 9.85 | 9.07 | 12 | Aspect ratio |
| 0.2 | 0.313 | 0.217 | 0.314 | 0.45 | Kink position |
| 25 | 27.1 | 31.6 | 27.1 | 45 | Sweep angle, deg |
| 0.4 | 0.598 | 0.459 | 0.495 | 0.7 | Inboard taper ratio |
| 0.2 | 0.506 | 0.202 | 0.273 | 0.6 | Outboard taper ratio |
| 0.1 | 0.150 | 0.174 | 0.177 | 0.18 | Root $t/c$ |
| 0.06 | 0.122 | 0.068 | 0.077 | 0.14 | Kink $t/c$ |
| 0.06 | 0.122 | 0.078 | 0.125 | 0.14 | Tip $t/c$ |
| 4.0 | 4.5 | 4.5 | 4.8 | 5.0 | Tip washout, deg |
| 0.65 | 0.75 | 0.66 | 0.75 | 0.84 | Kink washout fraction |
| | 191,879 | 190,582 | 187,703 | 135,000 | Wing weight, N |
| 40.0 | 42.35 | 40.8 | 45.5 | | Wing volume, m$^3$ |
| | 4.179 | 5.31 | 3.94 | 5.4 | Pitch-up margin |
| 2.5 | 2.693 | 3.84 | 3.34 | | Undercarriage bay length, m |
| | 3.12 | 2.75 | 3.02 | | Tadpole $D/q$, m$^2$ |
| | 2.85 | 2.37 | 2.54 | | MGAERO $D/q$, m$^2$ |

[a]Taken from Ref. 1.

**Table 9 Kriging hyperparameters for fused Tadpole/MGAERO model with 11 variables produced from 250 LP$\tau$ data points[a]**

| $\text{Log}_{10}(\theta)$ | $p_h$ | Quantity |
|---|---|---|
| _1.875 | 2.000 | Wing area |
| _3.795 | 1.999 | Aspect ratio |
| _8.414 | 1.858 | Kink position |
| 2.844 | 1.807 | Sweep angle |
| _1.381 | 1.003 | Inboard taper ratio |
| _7.707 | 1.058 | Outboard taper ratio |
| _9.603 | 1.033 | Root $t/c$ |
| _2.811 | 1.726 | Kink $t/c$ |
| _9.746 | 1.064 | Tip $t/c$ |
| _7.744 | 1.019 | Tip washout |
| _2.388 | 1.997 | Kink washout fraction |

[a]Regularization constant $= 2 \times 10^{-2}$.

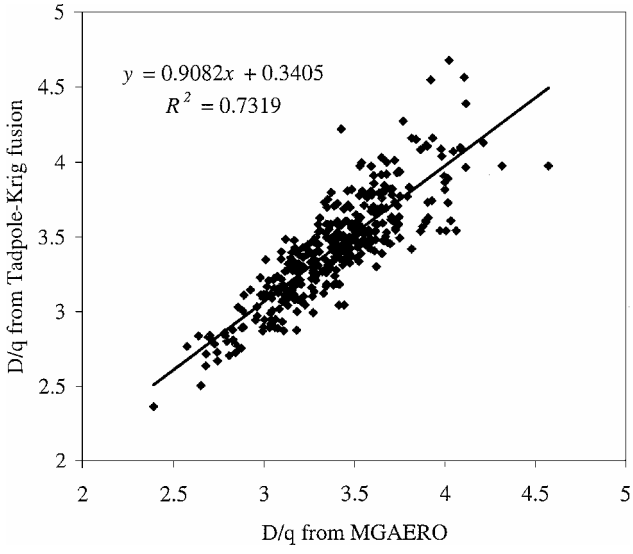


**Fig. 6 Correlation between 390 random MGAERO $D/q$ calculations and those predicted by the Tadpole–Kriging fusion trained on a separate set of 250 LP$\tau$ calculations.**

Again the model may be tested by its ability to predict unseen data. Figure 6 shows such a plot, where the same 390 results used earlier are compared with the drag values coming from direct calls to MGAERO. It may be seen that whereas significant differences do still occur, the overall correlation coefficient is now 0.7319 as compared to 0.4903 for the kriging, based solely on the MGAERO data. This improved predictive capability arises despite the mean SCV residual of the kriging being 1.224 with 22 of the 390 residuals being greater than three. This is because the kriging is now not used alone, but as a corrector to an already well set up empirical method, that is, a combination of black-box and physics-based estimators is being used, so that deficiencies in the kriging are compensated for by Tadpole and vice versa. The correlation coefficient measures the effectiveness of this combined process.

By use of this fusion model, optimization of the design being studied can be tried. Table 10 shows the results from using the model without any further updates, whereas Table 11 shows the results if 10 updates are added following the strategy already outlined.

Now the improvement in MGAERO drag before updates is almost as good as that from the direct search on the code, whereas after updates it is 0.3% better. Moreover, after the updates, the Tadpole drag is over 1% better than for the direct search on the Tadpole code at the same time. The final design is shown in Fig. 7. This optimization process again uses around one-sixth of the computing effort of the direct search on the CFD code.

It is interesting to compare the initial and final designs. The initial design has slightly greater area, less sweep, and much higher percentage of its lift generated by the outboard sections. Notice also that in Fig. 1 there is weakly supersonic flow over a large region of the upper surface (although there is virtually no wave drag on this design), whereas in Fig. 7 there is a much more localized but stronger shock near the wing tip. The impact of this shock on the overall drag is more than compensated for, however, by the large, low-drag inboard section of wing. Despite the shock, only 1.1% of the total drag on the design is wave drag. Note also that the optimized design is at the limits of two of the constraints: wing volume and pitch-up

**Table 10 Design parameters, constraint values, and objective function values for the best design produced by the search on the initial MGAERO/Tadpole difference kriging**

| Lower limit | Value | Upper limit | Quantity |
|---|---|---|---|
| 100 | 153.3 | 250 | Wing area, $m^2$ |
| 6 | 10.56 | 12 | Aspect ratio |
| 0.2 | 0.297 | 0.45 | Kink position |
| 25 | 27.04 | 45 | Sweep angle, deg |
| 0.4 | 0.424 | 0.7 | Inboard taper ratio |
| 0.2 | 0.201 | 0.6 | Outboard taper ratio |
| 0.1 | 0.129 | 0.18 | Root $t/c$ |
| 0.06 | 0.106 | 0.14 | Kink $t/c$ |
| 0.06 | 0.0820 | 0.14 | Tip $t/c$ |
| 4.0 | 4.054 | 5.0 | Tip washout, deg |
| 0.65 | 0.655 | 0.84 | Kink washout fraction |
| | 133,700 | 135,000 | Wing weight, N |
| 40.0 | 40.0 | | Wing volume, $m^3$ |
| | 4.61 | 5.4 | Pitch-up margin |
| 2.5 | 3.42 | | Undercarriage bay length, m |
| | 2.262 | | Kriging $D/q$, $m^2$ |
| | 2.875 | | Tadpole $D/q$, $m^2$ |
| | 2.531 | | MGAERO $D/q$, $m^2$ |

**Table 11 Final design parameters, constraint values and objective function values for the best design produced by the search on the refined MGAERO/Tadpole difference Krig produced with 10 updates and those for the initial design**

| Lower limit | Value | Upper limit | Quantity | Initial value from Table 1 |
|---|---|---|---|---|
| 100 | 156.6 | 250 | Wing area, $m^2$ | 168 |
| 6 | 10.25 | 12 | Aspect ratio | 9.07 |
| 0.2 | 0.436 | 0.45 | Kink position | 0.313 |
| 25 | 31.2 | 45 | Sweep angle, deg | 27.1 |
| 0.4 | 0.438 | 0.7 | Inboard taper ratio | 0.598 |
| 0.2 | 0.200 | 0.6 | Outboard taper ratio | 0.506 |
| 0.1 | 0.118 | 0.18 | Root $t/c$ | 0.150 |
| 0.06 | 0.124 | 0.14 | Kink $t/c$ | 0.122 |
| 0.06 | 0.0667 | 0.14 | Tip $t/c$ | 0.122 |
| 4.0 | 4.601 | 5.0 | Tip washout, deg | 4.5 |
| 0.65 | 0.717 | 0.84 | Kink washout fraction | 0.75 |
| | 128,888 | 135,000 | Wing weight, N | 127,984 |
| 40.0 | 40.1 | | Wing volume, $m^3$ | 41.73 |
| | 5.4 | 5.4 | Pitch-up margin | 4.179 |
| 2.5 | 2.96 | | Undercarriage bay length, m | 2.693 |
| | 2.012 | | Kriging $D/q$, $m^2$ | |
| | 2.817 | | Tadpole $D/q$, $m^2$ | 3.145 |
| | 2.515 | | MGAERO $D/q$, $m^2$ | 2.922 |

**Table 12 Summary of $D/q$ results**

| Table | Tadpole | % Table 1 | MGAERO | % Table 1 | Kriging | Notes |
|---|---|---|---|---|---|---|
| 1 | 3.145 | 100.0 | 2.922 | 100.0 | | Initial design |
| 2 | 2.853 | 90.7 | 2.555 | 87.4 | | Tadpole search |
| 3 | 2.998 | 95.3 | 2.524 | 86.4 | | MGAERO search |
| 6 | 3.046 | 96.9 | 2.777 | 95.0 | 2.429 | Kriging search |
| 7 | 2.879 | 91.5 | 2.543 | 87.0 | 2.316 | Kriging plus updates |
| 10 | 2.875 | 91.4 | 2.531 | 86.6 | 2.262 | Fusion kriging search |
| 11 | 2.817 | 89.6 | 2.515 | 86.1 | 2.012 | Fusion kriging plus update |
| 13 | 2.831 | 90.0 | 2.471 | 84.6 | 2.260 | Best design ever |

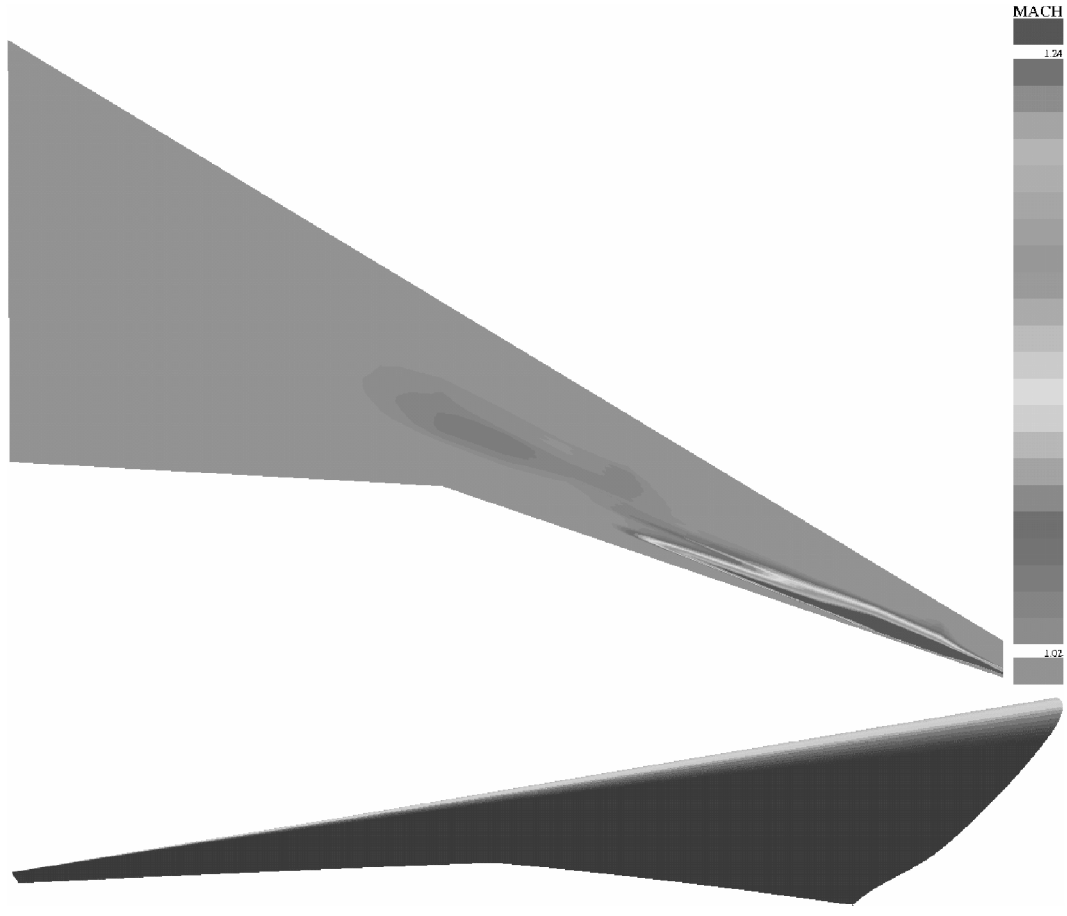


**Fig. 7 Geometry of final design produced by the search on the refined MGAERO/Tadpole difference kriging with 10 updates (plan view shows upper surface supersonic Mach contours).**

**Table 13 Final design parameters, constraint values and objective function values for the lowest MGAERO drag design found for the problem being searched**

| Lower limit | Value | Upper limit | Quantity |
|---|---|---|---|
| 100 | 147.6 | 250 | Wing area, $m^2$ |
| 6 | 11.20 | 12 | Aspect ratio |
| 0.2 | 0.436 | 0.45 | Kink position |
| 25 | 26.3 | 45 | Sweep angle, deg |
| 0.4 | 0.491 | 0.7 | Inboard taper ratio |
| 0.2 | 0.215 | 0.6 | Outboard taper ratio |
| 0.1 | 0.176 | 0.18 | Root $t/c$ |
| 0.06 | 0.0941 | 0.14 | Kink $t/c$ |
| 0.06 | 0.0605 | 0.14 | Tip $t/c$ |
| 4.0 | 4.992 | 5.0 | Tip washout, deg |
| 0.65 | 0.849 | 0.84 | Kink washout fraction |
| | 131,785 | 135,000 | Wing weight, N |
| 40.0 | 40.1 | | Wing volume, $m^3$ |
| | 4.75 | 5.4 | Pitch-up margin |
| 2.5 | 2.58 | | Undercarriage bay length, m |
| | 2.260 | | Kriging $D/q$, $m^2$ |
| | 2.831 | | Tadpole $D/q$, $m^2$ |
| | 2.471 | | MGAERO $D/q$, $m^2$ |

margin. This is a common feature in optimization processes and means that great care must be placed in setting the values of such hard constraints. The various drag values from all of the searches described here are summarized in Table 12 for ease of comparison.

Finally, remember that none of the designs produced using direct, simple RSM or fusion-based RSM searches can be guaranteed to be at the optimum of the problem being tackled: If different search strategies or starting points are employed, different optima can be located. Table 13 shows one such design that is better than all of those detailed so far from the MGAERO point of view. This design was in fact produced without using the Tadpole-based fusion strategy, although locating it was something of a fluke: It was found when testing the system described with all 640 MGAERO evaluations to build RSMs. Using bigger data sets is clearly an advantage when carrying out data modeling. It turns out to be 1.5% better than the design given by the fusion-based approach in terms of MGAERO predictions (but note that it is worse in terms of Tadpole drag calculations, as might be expected).

## Conclusions

Three distinct methods for carrying out aerodynamic design optimization are described: direct optimization of the user's analysis codes, search of a response surface derived from the user's codes, and search of a response surface derived from two related but different fidelity user codes. The latter multilevel or fusion-based approach seeks to combine the speed of fast empirical codes with the precision of full three-dimensional CFD solvers. This requires an integrated system of analysis that allows multiple codes to be used alongside each other: Here this is provided by the Southampton wing design system that has been described before.

In the study reported, the fusion-based approach is shown to outperform direct search of the CFD code at considerably reduced cost, while also being more accurate than a simple RSM using only data from the CFD code.

## Acknowledgments

Development of the Southampton wing design environment used here was supported by the U.K. Engineering and Physical Sciences Research Council under Grant GR/L04733 and by BAE Systems. Their support is gratefully acknowledged.

## References

[1]Keane, A. J., and Petruzzelli, N., "Aircraft Wing Design Using GA-Based Multilevel Strategies," AIAA Paper 2000-4937, Sept. 2000.

[2]Cousin, J., and Metcalfe, M., "The BAE Ltd. Transport Aircraft Synthesis and Optimization Program," AIAA Paper 90-3295, Sept. 1990

[3]Robinson, G. M., and Keane, A. J., "Concise Orthogonal Representation of Supercritical Airofoils," *Journal of Aircraft*, Vol. 38, No. 3, 2001, pp. 580–583.

[4]Harris, C. D., "NASA Supercritical Airfoils: A Matrix of Family-Related Airfoils," NASA TP 2969, March 1990.

[5]Mead, R., *The Design of Experiments*, Cambridge Univ. Press, Cambridge, England, U.K., 1988.

[6]Mackay, M. D., Beckman, R. J., and Conover, W. J., "A Comparison of Three Methods for Selecting Values of Input Variables in the Analysis of Output from a Computer Code," *Technometrics*, Vol. 21, 1979, pp. 239–245.

[7]Jones, D. R., Schonlau, M., and Welch, W. J., "Efficient Global Optimization of Expensive Black-box Functions," *Journal of Global Optimization*, Vol. 13, 1998, pp. 455–492.

[8]Myers, R. H., and Montgomery, D. C., *Response Surface Methodology: Process and Product Optimization Using Design of Experiments*, Wiley, New York, 1995.

[9]Alexandrov, N. M., Dennis, J. E., Lewis, R. M., and Torczon, V., "A Trust Region Framework for Managing the Use of Approximation Models in Optimisation," *Structural Optimization*, Vol. 15, 1998, pp. 16–23.

[10]Vitali, R., Haftka, R. T., and Sankar, B. V., "Multifidelity Design of Stiffened Composite Panel with a Crack," 4th World Congress of Structural and Multidisciplinary Optimization, Paper 51-AAM2-1, Buffalo, NY, May 1999.

[11]Malone, J. B., Housner, J. M., and Lytle, J. K., "The Design of Future Airbreathing Engine Systems Within an Intelligent Synthesis Environments," *Proceedings of the 14th International Symposium on Air Breathing Engines*, edited by P. J. Waltrup, Florence, 1999.

[12]Hutchinson, M. G., Unger, E. R., Mason, W. H., and Haftka, R. T., "Variable Complexity Aerodynamic Optimization of a High-Speed Civil Transport Wing," *Journal of Aircraft*, Vol. 31, No. 1, 1994, pp. 110–116.

[13]Liu, B., Haftka, R. T., and Akgün, M. A., "Two-Level Composite Wing Structural Optimization Using Response Surfaces," Structural Optimization, Vol. 20, No. 2, 2000, pp. 87–96.

[14]Zang, A. T., and Green, L. L., "Multidisciplinary Optimization Techniques: Implications and Opportunities for Fluid Dynamic Research," AIAA Paper 99-3798, Norfolk, VA, June 1999.

[15]Hutchison, M. G., Unger, E. R., Mason, W. H., Grossman, B., and Haftka, R. T., "Variable-Complexity Aerodynamic Optimization of a High-Speed Civil Transport Wing," *Journal of Aircraft*, Vol. 31, No. 1, 1994, pp. 110–116.

[16]Epstein, B., Luntz, A., and Nachson, A., "Multigrid Euler Solver About Aircraft Configurations, with Cartesian Grids and Local Refinement," AIAA Paper 89-1960, 1989.

[17]Lock, R. C., "Prediction of the Drag of Aerofoils and Wings at High Subsonic Speeds," *Aeronautical Journal*, June/July 1986, pp. 207–226.

[18]Squire, H. B., and Young, A. D., "The Calculation of Profile Drag of Aerofoils," Aeronautical Research Council, ARC R&M 1838, 1937.

[19]van Dam, C. P., and Nikfetrat, K., "Accurate Prediction of Drag Using Euler Methods," *Journal of Aircraft*, Vol. 29, No. 3, 1992, pp. 516–519.

[20]Goldberg, D. E., *Genetic Algorithms in Search, Optimization and Machine Learning*, Addison Wesley Longman, Reading, MA, 1989.

[21]Nelder, J. A., and Meade, R., "A Simplex Method for Function Minimization," *Computer Journal*, Vol. 7, 1965, pp. 308–313.

[22]Rosenbrock, H. H., "An Automatic Method for Finding the Greatest or Least Value of a Function," *Computer Journal*, Vol. 3, No. 3, 1960, pp. 175–184.

[23]Yin, X., and Germay, N., "A Fast Genetic Algorithm with Sharing Scheme Using Cluster Methods in Multimodal Function Optimization," *Proceedings of the International Conference on Artificial Nueral Nets and Genetic Algorithms*, edited by R. F. Albrecht, C. R. Reeves, and N. C. Steele, Springer-Verlag, Berlin, 1993, pp. 450–457.

[24]Anderberg, M. R., *Cluster Analysis for Applications*, Academic Press, New York, 1975.

[25]Statnikov, R. B., and Matusov, J. B., *Multicriteria Optimization and Engineering*, Chapman and Hall, New York, 1995.